Pore wall charge patterning and spatial profiles of electrical conductivity in short nanopores

M. Tajparast[1], M.I. Glavinovic[2]

Departments of [1]Civil Engineering and Applied Mechanics and [2]Physiology, McGill University, 3655 Sir William Osler Promenade, Montreal, QC, H3G 1Y6, Canada, mladen.glavinovic@mcgill.ca

ABSTRACT

Spatial distributions of conductivity and resistivity of short cylindrical nanopores were calculated from voltage and current profiles before and after small voltage perturbation. In narrow bi-polar nanopore with reverse bias the resistance is very high (its conductivity is very low), but diminishes more than expected based on geometry as pore widens due to the pronounced conductivity rise. In contrast if the bias is regular the conductivity is high, but diminishes as pore widens. If in bipolar nanopores the bias is regular the conductivity is higher than outside, and is axially highly non-uniform, especially near the wall, where it dips in the middle (i.e. where two oppositely charged halves meet). With reverse bias the conductivity is very low throughout the nanopore regardless of radial distance even for wide pores, and is much lower than outside.

Keywords: Navier-Stokes; Poisson-Nernst-Planck; Electrical conductivity; Nanopore

INTRODUCTION

Inspired by biological channels engineers now create artificial nanopores that serve as filters, nanofluidic switches or biosensors. Given that their functioning often depends on their conductivity it is important to determine how different factors, but especially the distribution of the pore wall charges and voltage bias influence the pore conductivity and its spatial distribution. Such an analysis would inform us how much the longitudinal and radial shrinkage of engineered nanopores is realistic. We focused our attention on two idealized cases - unipolar and bipolar short (10 nm in length) nanopores under either regular or reverse voltage bias. Short non-uniformly charged nanopores are very ubiquitous in nature functioning as biological ion channels and fusion pores, that link the vesicular interior with the extracellular space, and which provide a conduit for the secretion of the vesicular content [1]. The conductance of the fusion pores can change rapidly during extrusion of hormones, transmitters or peptides [2,3], but it is still not clear whether this is due to the change of the pore radius, or because the intra-vesicular transmitter and ion concentration change, or because the fixed charge density on the fusion pore wall changes due to the changes of the vesicular pH associated with the fusion pore opening.

The transport of ions and water through nanofluidic pores is governed by the concentration, potential and pressure gradients and better understanding of the interplay of these forces, and of the resulting ion fluxes is important to fully understand the mechanism of exocytosis of hormones, transmitters or peptides through the fusion pore. Finally, the characterization of the ion transport through short charged nanopores in terms of experimentally measurable variables (pore conductivity and resistivity) is desirable including the evaluation of their spatial distributions. We simulated the distribution and transport of charged particles (K^+, glutamate$^-$, Na^+ and Cl^-) in a charged nanofluidic pore using Poisson–Nernst–Planck equation. This is coupled to the transport of water using Navier–Stokes equations [4]. The computational domain consisted of a charged cylindrical pore flanked by two compartments (representing the vesicular interior and extra-cellular space), which were separated by a membrane. The simulations were done in the presence of the concentration, potential and pressure gradients between two compartments. The potential difference between two compartments was additionally perturbed, which allowed us to estimate the linear properties of electrical conductivity, resistivity and conductance and their spatial profiles [5,6].

METHODS

1.1 Mathematical model

Poisson-Nernst-Planck (PNP) equations are used to calculate ionic current through a pore for all charged species. The electrostatic potential (Φ) is calculated using Poisson equation:

$$-\nabla.\varepsilon_0\varepsilon_r\nabla\Phi=\rho_e \quad (1)$$

where ε_0 is the permittivity of vacuum, ε_r is the relative dielectric constant of solution. In the membrane the relative dielectric constant is ε_m, and the charge density ρ is zero. In solution the charge density ρ_e is given by:

$$\rho_e = F\sum z_a c_a \left(= e\sum z_a n_a\right) \quad (2)$$

where c_a is the molar concentration of ion a [mol/m^3], F is Faraday constant (9.648×10^4 C/mol), z_a is the valence of ion a, n_a is the number density of ion a. The potential in the pore is influenced by: a) the fixed charges on the pore wall, b) the mobile charges inside the pore, and c) the charges in the solution and on control edges outside the pore.

The movement (by convection-diffusion-migration) of ionic species in the solution is given by the Nernst-Planck equation:

$$\mathbf{J_a} = \mathbf{u}c_a - D_a\nabla c_a - m_a z_a F c_a \nabla\Phi \quad (3)$$

where $\mathbf{J_a}$ is molar flux [mol/m^{2}s], D_a and m_a are diffusivity and mobility of ion a ($m_a = D_a/RT$), respectively; **u** is fluid velocity and F, R and T are Faraday constant, gas constant [8.314 J/(Kmol)] and temperature (in Kelvin), respectively. The conservation of ionic mass is given by:

$$\frac{\partial c_a}{\partial t} + \nabla.\mathbf{J_a} = 0 \quad (4)$$

The fluid velocity **u** is computed from the time dependent Navier-Stokes (NS) equations:

$$\rho\left(\frac{\partial\mathbf{u}}{\partial t} + \mathbf{u}.\nabla\mathbf{u}\right) = -\nabla p + \nabla.\left[\mu\left[\nabla\mathbf{u} + (\nabla\mathbf{u})^T\right]\right] + \mathbf{F_e} \quad (5)$$

$$\nabla.\mathbf{u} = 0 \quad (6)$$

Equation (5) describes the conservation of momentum, while equation (6) accounts for the conservation of mass. In these equations ρ_f, μ, and p are respectively the density, viscosity and pressure of the fluid, while $\mathbf{F_e}$ is the electric force per unit volume ($\mathbf{F_e} = \rho_e\nabla\Phi$).

1.2 Geometry, parameters and boundary conditions

The computational domain consists of the fusion pore, a piece of the membrane and the vesicular and extra-cellular space (Fig. 1). The length of the pore L and of vesicular and extra-cellular compartments was 10 nm. The pore radius R was 3 nm (but could range from 1 nm to 4 nm), whereas the radius W of the vesicular and extracellular compartments was 11 nm.

Axial symmetry condition is applied on all variables along the pore axis (Fig. 1). The boundary conditions for the Nernst-Planck equation are concentrations of K^+, glutamate$^-$, Na^+ and Cl^- on two external controlling edges of the upper or vesicular compartment and lower or extra-cellular compartment. On the edges of the upper compartment the concentrations of K^+ and glutamate$^-$ were 150 mM (mol/m^3), whilst the concentrations of Na^+ and Cl^- were 0 mM. On the edges of the lower compartment the concentrations of K^+ and glutamate$^-$ were 0 mM, while the concentration of Na^+ and Cl^- were 150 mM. We assume that: a) glutamate is negatively charged, with a single negative charge, which remains constant throughout simulations, b) glutamate is an ion (anion; i.e. the complexities of its shape are ignored). At the solution-membrane interface an insulation/symmetry condition was imposed. On the upper and lower controlling edges the potential was as indicated. On the internal wall of the pore (including the curved parts) the surface charge density (σ) was as shown, but ranged from 0 to +64 mC/m^2. These values are within the range of values estimated for the cell membrane [7]. On the membrane exterior walls the surface charge density was 0 C/m^2. Finally, no-penetration and no-slip condition was imposed on the solution-membrane interface. The pressure at the upper controlling edges was 0 kPa or 500 kPa, whereas at the lower controlling edges it was 0 kPa. The relative dielectric constants of the membrane (e_m) and solution (ε_s) were 2 and 80 respectively. The diffusion constants of Na^+, Cl^-, K^+ and glutamate$^-$ were 1.33×10^{-9}, 2.03×10^{-9}, 1.96×10^{-9}, and 0.76×10^{-9} m^2/s [8], respectively, the viscosity of the fluid was 1 mPas, and the temperature was 300 K. The system of coupled PNP-NS equations was solved by finite element method using Comsol 4.3a (Comsol, Burlington, MA, USA), and the post-processing using Matlab (MathWorks, Natick, MA, USA).

RESULTS

2.1 Radial profiles of resistivity and conductivity in a unipolar nanopore with 'Reverse Bias'

Fig. 1 (top panels) depicts three color-coded 2D distributions of the potential in the nanopore, two compartments flanking it and in the piece of membrane separating the compartments (left panel), of the co-ion and of the counter-ion concentration within the pore (middle and right panels respectively). Figs. 1A-B give the radial profiles of the differential of voltage difference (total dVd as well as those of its two halves; note that the dVd of the charged half is smaller), and of the differential of

current density (dId) respectively. Figs. 1C-D give the resistivity (Note that in the charged half it is ~50% of that in the uncharged half) and the total conductivity profiles respectively. In both - the charged and uncharged half - the resistivity is lower near the wall.

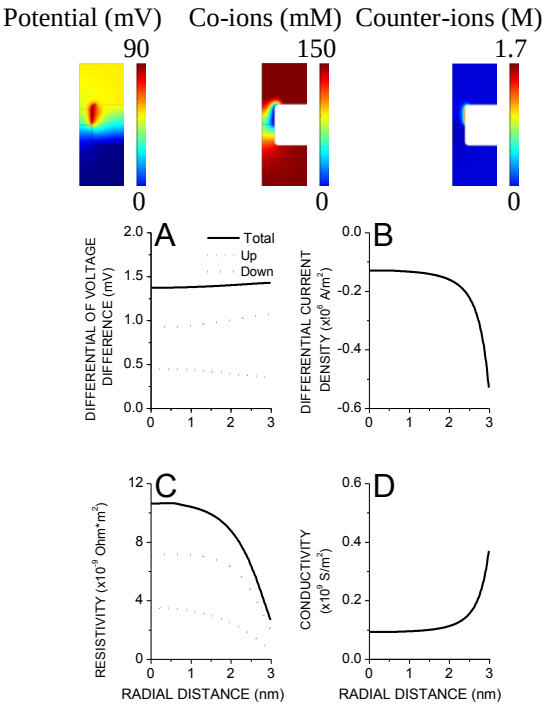

Fig. 1. 2D color coded distributions of the potential, co-ion and counter-ion concentrations. Calibration bars are as indicated. The top, middle and bottom virtual lines in the pore depict where the various variables (potential, current, current density) are evaluated. A) Differential of voltage difference (dVd). B) Differential of current density (dId). C) Resistivity. D) Conductivity. V_u=0mV (or 2mV) and V_d=0mV.

2.2 Conductivity profiles of bipolar nanopores

Fig. 2 depicts 3D distribution of the conductivity within and outside of the narrow (left panels) and wide (right panels) bipolar nanopores (Regular bias - upper panels; Reverse bias - lower panels) together with the corresponding families of axial profiles (same data; Figs. $2A_1$-A_2 and $2B_1$-B_2). Note that with the regular bias the conductivity is clearly higher within the pore than outside, but shows a dip in the middle where two oppositely charged halves meet. In contrast if the bias is reverse the conductivity within the nanopore is far below that outside, and is the lowest near the wall.

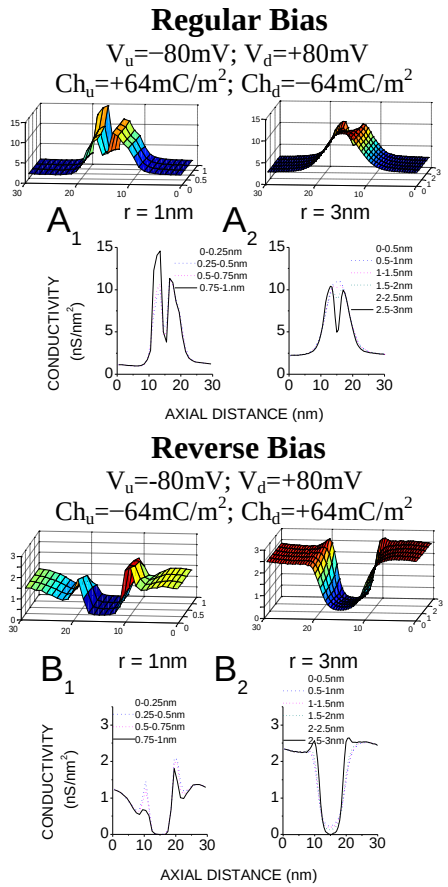

Fig. 2. Conductivity 3D color coded profiles for a narrow (r=1nm; left panels) and wide (r=3nm; right panels) bipolar nanopores together with the corresponding families of the axial profiles (same data). Regular bias (top panels and Figs. $2A_1$-A_2). Reverse bias (bottom panels and Figs. $2B_1$-B_2).

2.3 Radius dependence of resistance and conductivity of bipolar nanopores

Fig. 3A shows the resistance vs. radius relationship of the short cylindrical bipolar nanopore. The resistance is low and diminishes with radius, but only modestly if the bias is regular. If it is reverse the resistance is much higher, but diminishes greatly with radius. This is due to the changes of conductivity. If the bias is regular the conductivity is high and diminishes, though very modestly as radius increases, but if the bias is reverse the conductivity is much lower but rises markedly as pore widens (Fig. 3B).

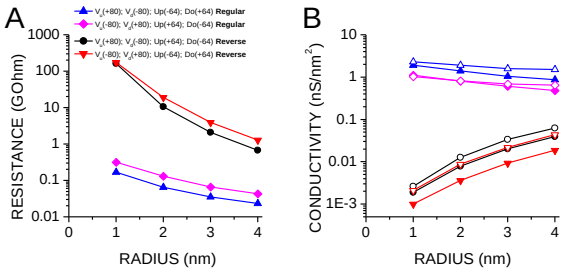

Fig. 3. A) Resistance vs. radius relationship, and B) conductivity vs. radius relationship. Regular bias (blue and purple symbols); Reverse bias (Red and black symbols). Open symbols - near wall; filled symbols - pore center.

DISCUSSION

The physics of the problem was described by a coupled set of electrostatic/electrokinetic (Poisson–Nernst–Planck) and fluidic (Navier–Stokes) equations in a computational domain consisting of a short cylindrical nanopore flanked by the vesicular and extra-cellular compartments, which are separated by a piece of membrane. Based on these simulations we calculated the spatial profiles of the linear electrical properties of the charged nanopore. They were calculated from the voltage and current profiles before and after perturbation of the voltage difference between two compartments flanking the nanopore.

The resistance vs. radius and conductivity vs. radius relationships of the bipolar nanopores are quite complex. If the conductivity of the narrow bipolar nanopore is high, it will decrease as radius increases, but if it is low it will increase markedly. Whether the conductivity of the narrow nanopore is high or low depends on the voltage bias. Regular bias results in high and reverse bias in very low conductivity. Given this conductivity vs. radius relationship it is not surprising that with the reverse bias the resistance of bipolar nanopores is not only high, but that it also decreases greatly as pore widens. In contrast with regular voltage bias the resistance is not only lower, it also diminishes less as the pore widens.

This study also demonstrates that the resistivity of different parts of the nanopore is not necessarily the same. We evaluated how they contribute to the total resistance of the nanopore, and what possible ion transport bottlenecks (areas of high resistivity) may exist. We first estimated the radial resistivity (and conductivity) profiles for the whole unipolar nanopore (under reverse bias) and for each of its halves. The resistivity of two halves is not the same, charged half having the lower resistivity. We also evaluated the spatial conductivity profiles of a narrow (r=1nm) and a wide (r=3nm) bipolar nanopore, under either regular or reverse bias. In bipolar nanopores under regular bias the conductivity (and thus the resistivity also) of two halves is quite similar, higher than outside of the nanopore, and higher near the wall. However, the axial non-uniformity of the conductivity is very pronounced, especially near the wall. In the middle of the nanopore (where two oppositely charged halves meet) there is a conductivity dip, which is especially pronounced in narrow pores. When the bias becomes reverse the conductivity within the nanopore becomes much lower throughout the nanopore, even when the nanopore is wide. It is also much lower than outside of the nanopore.

Note however that in these simulations we assume that the diffusion constants of the charged particles (K^+, glutamate$^-$, Na^+ and Cl^-) are independent of their position in the simulation space (i.e. the diffusive properties are considered to be homogeneous in the nanopore and in both compartments flanking it). This is an over-simplification because molecular dynamics simulations have shown that the diffusive properties of ions and charged particles are quite inhomogeneous within the nanopore. The diffusive constants can be much lower near the pore wall [9], and this would alter the pore resistance and the spatial distribution of electrical properties of the nanopore.

REFERENCES

[1] D. Sulzer, E.N. Pothos (2000) Rev. Neurosci. 11, 159–212.
[2] L.J. Breckenridge, W. Almers (1987) Nature 328, 814–817.
[3] L.J. Breckenridge, W. Almers (1987) Proc. Natl. Acad. Sci. U. S. A. 84, 1945–1949.
[4] A. J. Grodzinsky. Fields, forces and flows in biological systems, Garland Science, 2011.
[5] E. Brunet, A. Ajdari (2004) Phys. Rev. E 69, 016306-2 – 016306-9.
[6] F.H.J. van der Heyden, D.J. Bonthuis, D. Stein, C. Meyer, C. Dekker (2006) Nano Lett. 6, 2232-2237.
[7] S.G.A. McLaughlin, G. Szabo, G. Eisenman (1971) J. Gen. Physiol. 58, 667–687.
[8] B. Hille, A.M. Woodhull, B.I. Shapiro (1975) Phil.. Trans. R. Soc. Lond., B. 270, 301–318.
[9] S.M. Cory, Y. Liu, M.I. Glavinović (2007) Biochim. et Biophys. Acta 1768, 2319–2341